General Disclaimer

One or more of the Following Statements may affect this Document

- This document has been reproduced from the best copy furnished by the organizational source. It is being released in the interest of making available as much information as possible.
- This document may contain data, which exceeds the sheet parameters. It was furnished in this condition by the organizational source and is the best copy available.
- This document may contain tone-on-tone or color graphs, charts and/or pictures, which have been reproduced in black and white.
- This document is paginated as submitted by the original source.
- Portions of this document are not fully legible due to the historical nature of some of the material. However, it is the best reproduction available from the original submission.

Produced by the NASA Center for Aerospace Information (CASI)

X-621-71-354

PREPRINT

NASA TM X- 65690

A POSSIBILITY OF MULTIPLE EXOSPHERIC TEMPERATURES FOR VENUS AND MARS

J. R. HERMAN

SEP 1971
RECEIVED

SEPTEMBER 1971

GSFC — GODDARD SPACE FLIGHT CENTER
GREENBELT, MARYLAND

FACILITY FORM 602

N71-36154 (ACCESSION NUMBER)	(THRU)
17 (PAGES)	G3 (CODE)
TMX-65690 (NASA CR OR TMX OR AD NUMBER)	30 (CATEGORY)

MULTIPLE EXOSPHERIC TEMPERATURES FOR VENUS AND MARS

by

J. R. Herman

Laboratory for Planetary Atmospheres
Goddard Space Flight Center
Greenbelt, Maryland 20771

MULTIPLE EXOSPHERIC TEMPERATURES FOR VENUS AND MARS

ABSTRACT

Solutions of the heat transport equations for each of the important neutral species in the upper atmosphere of Venus and Mars have shown that multiple neutral temperatures must be considered to properly understand the distribution of atomic hydrogen. Temperature differences between CO_2 and the light atomic species, H, D, and He in excess of 100 °K for Venus and 50 °K for Mars are obtained above the exobase. The magnitude and separation of these temperatures depend strongly on the relative proportion of light neutrals to carbon dioxide in the lower atmosphere and on the degree of turbulent mixing in the lower thermosphere (above 100 km). Since the atomic hydrogen effusion flux is strongly dependent on the exobase temperature, the exospheric hydrogen density is found to be very different from that based on the CO_2 temperature. The exospheric atomic hydrogen density is found to have a power law dependence on the proportion of neutral helium present in the atmosphere.

MULTIPLE EXOSPHERIC TEMPERATURES FOR VENUS AND MARS

The detailed knowledge we have of the neutral gas temperature above 100 km has been obtained from the Mariner and Venera series of flights to Venus and Mars. The Lyman α measurements made by *Barth et. al (1968, 1971)* and *Kurt, et. al (1968)* when coupled with an appropriate model of an exosphere, *Wallace (1969)* can be made to yield hydrogen temperatures and densities at high altitudes. Additional data can be obtained from electron density profiles such as the familiar data obtained by Mariner V, *Fjeldbo and Eshleman (1969)*. The neutral gas temperature can be inferred from the slope of the density profile above the ionization peak, Figure 1, if the atmospheric composition or mean mass is known. The procedure is valid because below about 180 km altitude the electron, ion, and neutral gases exhibit strong collisional coupling. This coupling both forces a common temperature $T_n \simeq T_i$ and minimizes the effects of ion-electron diffusion on the electron density scale height. Thus, the small scale height above the ionization peak has been used to infer a mainly CO_2^+ lower ionosphere in a CO_2 atmosphere with an exospheric temperature of 650 °K for Venus and 400 °K for Mars. Since the rapid change in scale height above 200 km on Venus clearly indicates a change in composition from CO_2 to light neutral gases, do the exospheric temperatures obtained from the electron density data also apply to the light atomic species He, H, and D at high altitudes? It will be shown that the general answer is no; the temperatures for CO_2 and the light gases are different except for certain special cases of atmospheric composition.

The computation of the temperatures was performed by the methods given in a recent paper by *Herman, et. al (1971)* with the addition of an independent heat flow equation for the light neutral gases, H, D, and He. Since the thermal behavior of these gases is quite similar it was decided to assign a common temperature to H, D, and He, but not to the heavier molecular gases such as CO_2. For example the thermal conductivities of H, D, and He are $16.4T^{0.73}$, $11.7T^{0.73}$, and $20.9T^{0.75}$ erg cm^{-1} sec^{-1} °K^{-1} respectively, and for CO_2 it is $1.50T^{1.23}$, *Tsederberg (1965)*. The heat input and loss mechanisms for H, D, and He are quite similar since they are dependent on electron-neutral, ion-neutral and neutral-neutral collisions rather than radiative processes as with CO_2. Thus, even though the absolute magnitudes of conduction, heating, and cooling rates may differ for H, D, and He, their functional dependencies and regions of importance are nearly the same in contrast with the very different behavior of CO_2. The heat sources used in the computations include solar EUV and solar wind heating as well as the important heat sources from the electron and ion gases.

Since CO_2 has a very small scale height both the heat input and loss is mainly confined below 150 km altitude with the result that the CO_2 exospheric temperature is determined almost entirely by the properties of this region. The light atomic species absorb energy in a comparitively uniform manner with altitude because of their large scale heights above the turbulent region in the atmosphere. For these gases, the heat energy must be conducted downward into the region of strong collisional coupling where it can be either transferred to the CO_2 and lost by infrared radiation or conduction into the dense atmosphere below. The details of the heat energy flow depend on whether the temperature of the light atomic species is greater or less than the CO_2 temperature. Above approximately 150 km the collisional coupling is weak so that the neutral gas temperature for He, H, and D is in part determined by the relative abundance of these species with respect to CO_2. An example of the temperature separation between the light and CO_2 gases is shown in Figure 2 for the diurnal variation of temperature and density in the Martian ionosphere at 200 km altitude corresponding to the conditions seen by Mariner VI at the latitude 4 ° north. The data points for Mariner VI are shown by the small rectangles labelled M6 and are clearly in good agreement with the computed ionospheric model (see Appendix). The diurnal neutral gas temperature variation is shown by the curves labelled T_n and T_L. For these conditions, T_n (the CO_2 temperature) becomes larger than T_L (the common H, D, and He temperature) shortly after sunrise and stays larger until well after sunset. From Figure 2 the time constant for thermal equilibrium is estimated to be about three hours. A similar plot for the diurnal variation on Venus differs only in the magnitude of the temperature separation and the lack of noticeable asymmetry about local noon because of the very slow rotation rate of Venus.

The temperature separation shown in Figure 2 has an obvious bearing on the problems of planetary evolution through the escape rate of hydrogen and on the present altitude distribution of hydrogen. For example, the effect of escaping hydrogen is illustrated in the relative behavior of H^+ and D^+ shortly after sunrise. On Mars with its weak gravity the normal exobase temperature is high enough so that hydrogen is depleted and D^+ is able to dominate H^+ throughout the day. The addition of O^+ to the ionosphere does not change their relative behavior. The rapid loss of H^+ and D^+ and the low density of He^+ (less than 10^3 cm^{-3}) as the day progresses is due to the mutual charge exchange reactions between the various ions and their neutral counterparts. The net result being that at 200 km altitude most of the produced ionization goes into the creation of additional CO_2^+. At higher altitudes other ions can dominate (H^+, D^+, or O^+) except for He^+ which remains a minor ion by charge exchange with all other neutral gases in the atmosphere.

On Venus the temperature separation can be critical for hydrogen escape. Even a 50 °K change in the gas temperature would be sufficient to substantially deplete the exosphere of Venus of hydrogen gas. An evaluation of the Jeans - effusion velocity (bulk velocity) $V_j = (kT_L/2\pi_H g)^{1/2} \quad (1 + R/H) \; \exp(-R/H)$ shows a strong temperature dependence ($V_j = 3.017\ (T/500)^{13.8755*}$) in the temperature range between 300 and 700 °K. R = the radial distance to the exobase, $H = kT_L/m_H g$, m_H = the mass of hydrogen, and g = the acceleration of gravity. Possible daytime temperature profiles for Venus and Mars are presented in Figure 3 showing a substantial temperature separation in the Venus exosphere. The magnitudes of the temperatures and their separation are controlled by the amount of light neutral gases present in upper atmosphere (above about 150 km). Since He^+ and He are free parameters at the present state of knowledge, the concentration of neutral helium below 100 km was varied to investigate its influence on the temperature and escape of atomic hydrogen, Figure 4. As the proportion of helium in the atmosphere below 100 km is increased the amount of solar EUV energy available for heating increases for the light neutrals and decreases for CO_2. In response to this, the light neutral temperature $T_n(H)$ rises while that of CO_2 decreases. The increase in $T_n(H)$ at 150 km is limited by the collisional coupling to CO_2. At first $T_n(H)$ increases rapidly but as $T_n(H)$ approaches $T_n(CO_2)$ and then exceeds it, the heat transfer from CO_2 decreases and finally becomes a heat loss. At 500 km,

* A least squares fit to V_j with a correlation coefficient greater than 0.99

however, where the collisional coupling is very small, the $T_n(H)$ and $T_n(CO_2)$ are uncoupled and $T_n(H)$ increases exponentially as a function of the atmospheric helium content. The effect on the hydrogen density N(H) is shown in Figure 5 as a power law decrease due to the increased hydrogen escape flux.* The details of the behavior of $T_n(H)$ and N(H) as shown in Figures 4 and 5 depends strongly on the degree of turbulent diffusion in the atmosphere below the turbopause region. As the degree of turbulent diffusion increases, as measured by an eddy diffusion coefficient (K_{eddy}), the minor constituents are forced to follow the CO_2 scale height to greater altitudes, *McElroy and Hunten (1969)* and *Herman et. al (1971)*. This results in a decrease in the density of light neutrals above the turbopause and a consequent decrease in $T_n(H)$ and an increase in $T_n(CO_2)$, Figure 6. Furthermore, when K_{eddy} is small $T_n(CO_2) > T_n(H)$ at 150 km and $T_n(CO_2) < T_n(H)$ at 500 km with a relatively small temperature separation, but for large K_{eddy} $T_n(H)$ decreases sharply and the temperature separation becomes very significant. The corresponding changes in the hydrogen densities are shown in Figure 7. As expected the decreasing $T_n(H)$ as K_{eddy} increases leads to a decrease in the hydrogen escape flux and to an increase in N(H). Further increases in K_{eddy} cause a decrease in N(H) because the decreasing outward bulk flow of hydrogen is eventually dominated by the turbulent mixing (i.e. the increase in altitude of the turbopause region).

For the case of the earth a similar temperature separation occurs between the H and He and the other atmospheric constituents (e.g. N_2, O_2, and O). However, the separation turns out to be small since the principal constituent for heat loss by infrared radiation, atomic oxygen, extends to great heights and provides good collisional coupling with H and He well into the region where the neutral gas temperatures are nearly isothermal.

* $[H]_{500} = 2.1 \times 10^{8} [He]_{100}^{-0.22}$

In conclusion, it has been shown that a multiple temperature neutral atmosphere must be considered for Venus and Mars (and to a much lesser extent on Earth) in the interpretation of data obtained from planetary probes. The temperature differences between the light atomic species (H, D, and He) and CO_2 are significant and, particularly on Venus, are very important in determining the escape flux of atomic hydrogen and its density above the turbopause region. In addition, the Lyman α determination of hydrogen density and temperature at great heights, *Barth (1968)* leads to an estimate of the Venus helium concentration at 100 km of 5×10^{8} cm^{-3} and a small value of the eddy diffusion coefficient (less than 5×10^{5} cm^{2} sec^{-1}).

APPENDIX

The computations performed in this work were obtained by simultaneously solving the equations of heat transport for each of the electron, ion, and neutral gases present in the atmosphere in the manner described by *Herman et. al (1971)* and *Herman and Chandra (1969)*. In addition the time dependent momentum and continuity equations were included to obtain the diurnal variation of densities and temperatures presented in Figure 2. A brief summary of these equations is as follows.

For each species, i, the momentum and continuity equations have the form

$$M_i N_i \frac{\partial V_i}{\partial t} + V_i \frac{\partial V_i}{\partial z} = - \frac{\partial P_i}{\partial z} - N_i M_i g + e_i N_i E - \sum_j K_{ij} (V_i - V_j)$$

$$\frac{\partial N_i}{\partial t} + \frac{\partial}{\partial z} (V_i N_i) = R_i - L_{Pi}$$

where the symbols all have their standard meaning. The quantity K_{ij} can be written in terms of collision frequency ν_{ij} as $K_{ij} = N_i N_j \mu_{ij} \nu_{ij}$ where μ_{ij} is the reduced mass. The electric field E is determined from the momentum equation for electrons (i.e. $N_i \rightarrow N_e$ and $e_i \rightarrow -|e|$). The ion production function R_i is the sum of ionization sources from the solar EUV, solar wind proton penetration of the ionosphere directly and via charge exchange with the ambient neutral atmosphere at great heights, and the mutual charge exchange between the various ions and the atmospheric gases. The loss function L_{pi} is the sum of the appropriate charge transfer and electron recombination terms for each ionic species.

REFERENCES

Barth, C. A., Wallace, L., and Pearce, J. B., Mariner 5 Measurement of Lyman Alpha Radiation near Venus, J. Geophys. Res., 73, 2541 (1968).

Barth, C. A., Hord, C. W., Pearce, J. B., Kelly, K. K., Anderson, G. P., and Stewart, A. I., Mariner 6 and 7 Ultraviolet Spectrometer Experiment: Upper Atmospheric Data, J. Geophys.Res., 76, 2213 (1971).

Fjeldbo, G. and Eshleman, V. R., Atmosphere of Venus as Studied with the Mariner 5 Dual Radio Frequency Occultation Experiment, Radio Sci., 4, 879 (1969).

Herman, J. R. and Chandra, S., The Influence of Varying Solar Flux on Ionospheric Temperatures and Densities: A Theoretical Study, Planet. Space Sci., 17, 815 (1969).

Herman, J. R., Hartle, R. E., and Bauer, S. J., The Dayside Ionosphere of Venus, Planet. Space Sci., 19, 443, (1971).

Kurt, V. G., Dostovalow, S. B., and Sheffer, E. K., The Venus far Ultraviolet Observations with Venera 4, J. Atmos. Sci., 25, 668 (1968).

McElroy, M. B. and Hunten, D. M., The Ratio of Deuterium to Hydrogen in the Venus Atmosphere, J. Geophys. Res., 74, 1720 (1969).

Tsederberg, N. V., Thermal Conductivity of Gases and Liquids, MIT Press, Cambridge, Massachusetts (1965).

Wallace, L., Analysis of Lyman Alpha Observations of Venus Made from Mariner 5, J. Geophys. Res., 74, 115 (1969).

FIGURE CAPTIONS

1 - Venus Dayside and Nightside Ionization Profiles. Taken from Fjeldbo and Eshleman (1969)

2 - The diurnal variation of temperatures and densities for Mars computed for conditions corresponding to Mariner VI. (4° N latitude, solar zenith angle 57°, and orbital longitude 284° with solar fluxes scaled to correspond to 7/31/69). The time scale is subdivided into 20 Mars hours of 4431 seconds each so as to divide evenly into a Mars day of 88620 seconds. On this scale hour 13 is equivalent to an Earth hour of 15.6. Solid rectangles labelled M6 represent Mariner VI data points.

3 - Daytime neutral gas temperatures for H, D, He, and CO_2 for Venus and Mars. Solar zenith angles and solar activity are the same for both planets.

4 - Daytime Venus CO_2 and H temperatures as a function of the helium concentration in the lower atmosphere (below 100 km). The dashed lines correspond to an altitude of 150 km and the solid lines to 500 km.

5 - Daytime Venus H densities at 150 km (dashed lines) and 500 km (solid lines) as a function of neutral helium concentration at 100 km altitude.

6 - Daytime Venus CO_2 and H temperatures as a function of the eddy diffusion coefficient. Dashed lines are at 150 km and solid lines at 500 km.

7 - Daytime Venus H densities at 150 km (dashed lines) and 500 km (solid lines) as a function of the eddy diffusion coefficient.

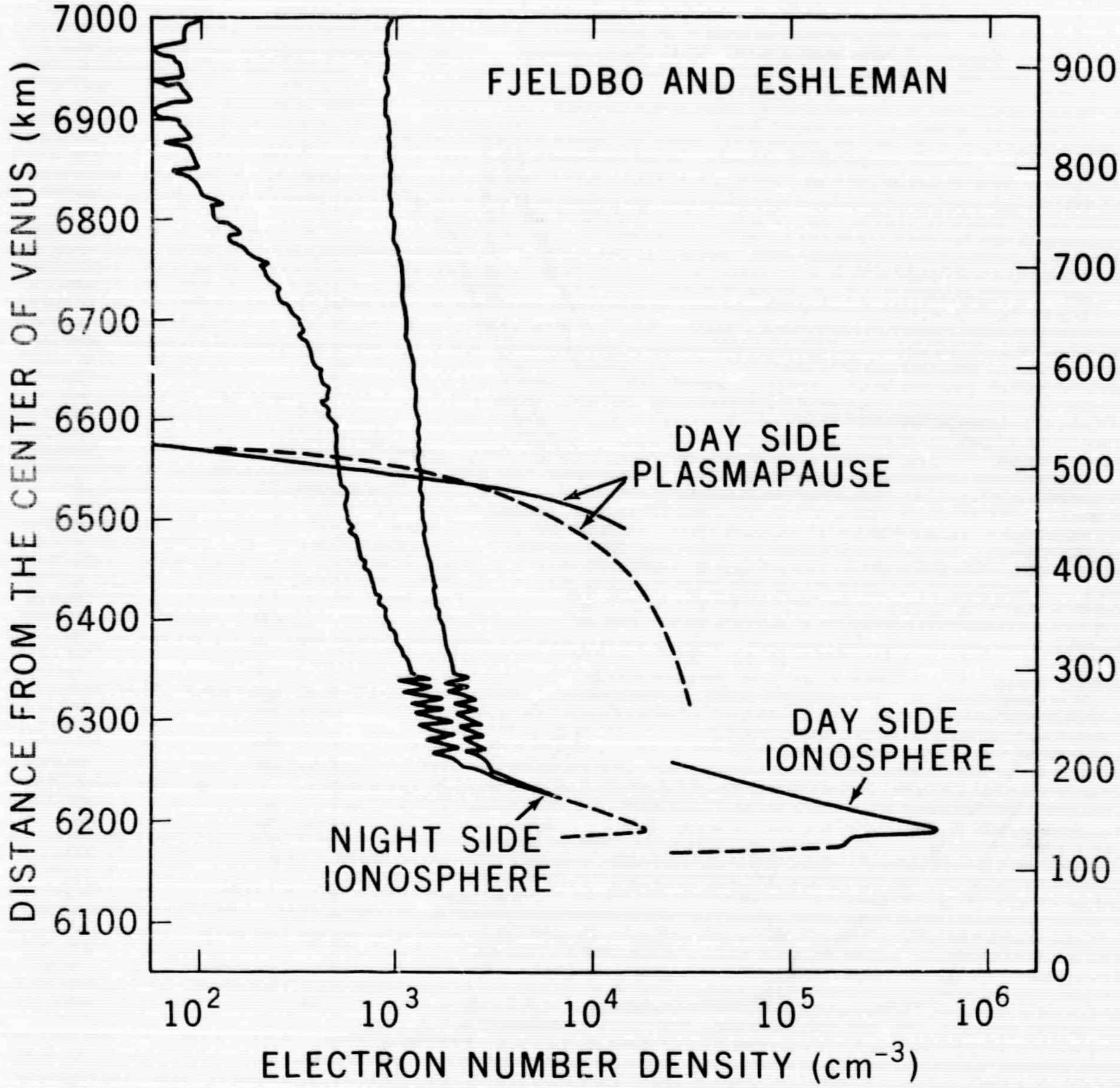

FJELDBO AND ESHLEMAN
DAY SIDE
PLASMAPAUSE
DAY SIDE
IONOSPHERE
NIGHT SIDE
IONOSPHERE
7000
6900
6800
6700
6600
6500
6400
6300
6200
6100
DISTANCE FROM THE CENTER OF VENUS (km)
900
800
700
600
500
400
300
200
100
0
ALTITUDE (km)
10^2
10^3
10^4
10^5
10^6
ELECTRON NUMBER DENSITY (cm^{-3})

Figure 1

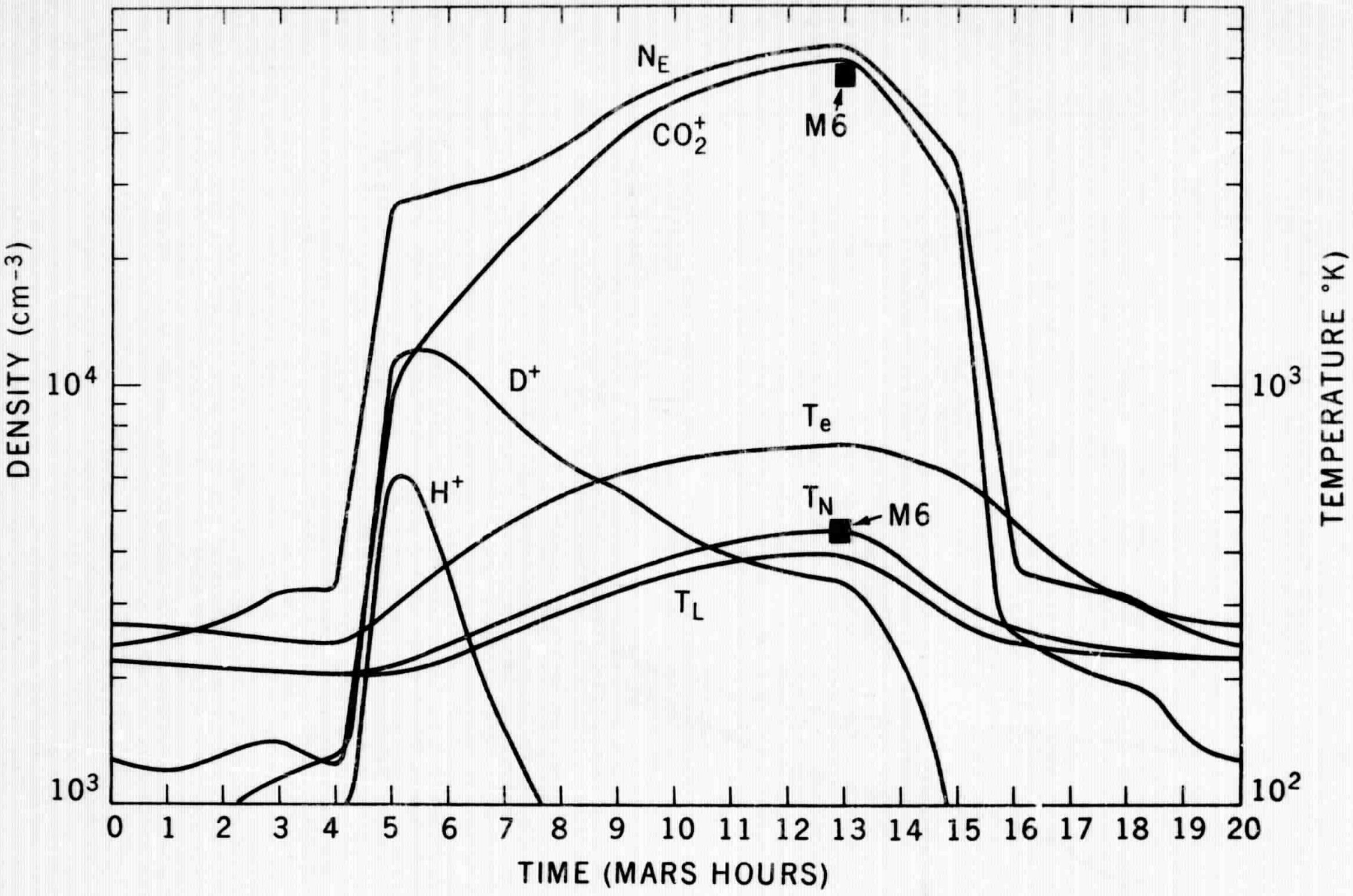

N_E
CO_2^+
M6
D^+
T_e
H^+
T_N
M6
T_L
DENSITY (cm-3)
TEMPERATURE °K)
10^4
10^3
10^3
10^2
0 1 2 3 4 5 6 7 8 9 10 11 12 13 14 15 16 17 18 19 20
TIME (MARS HOURS)

Figure 2

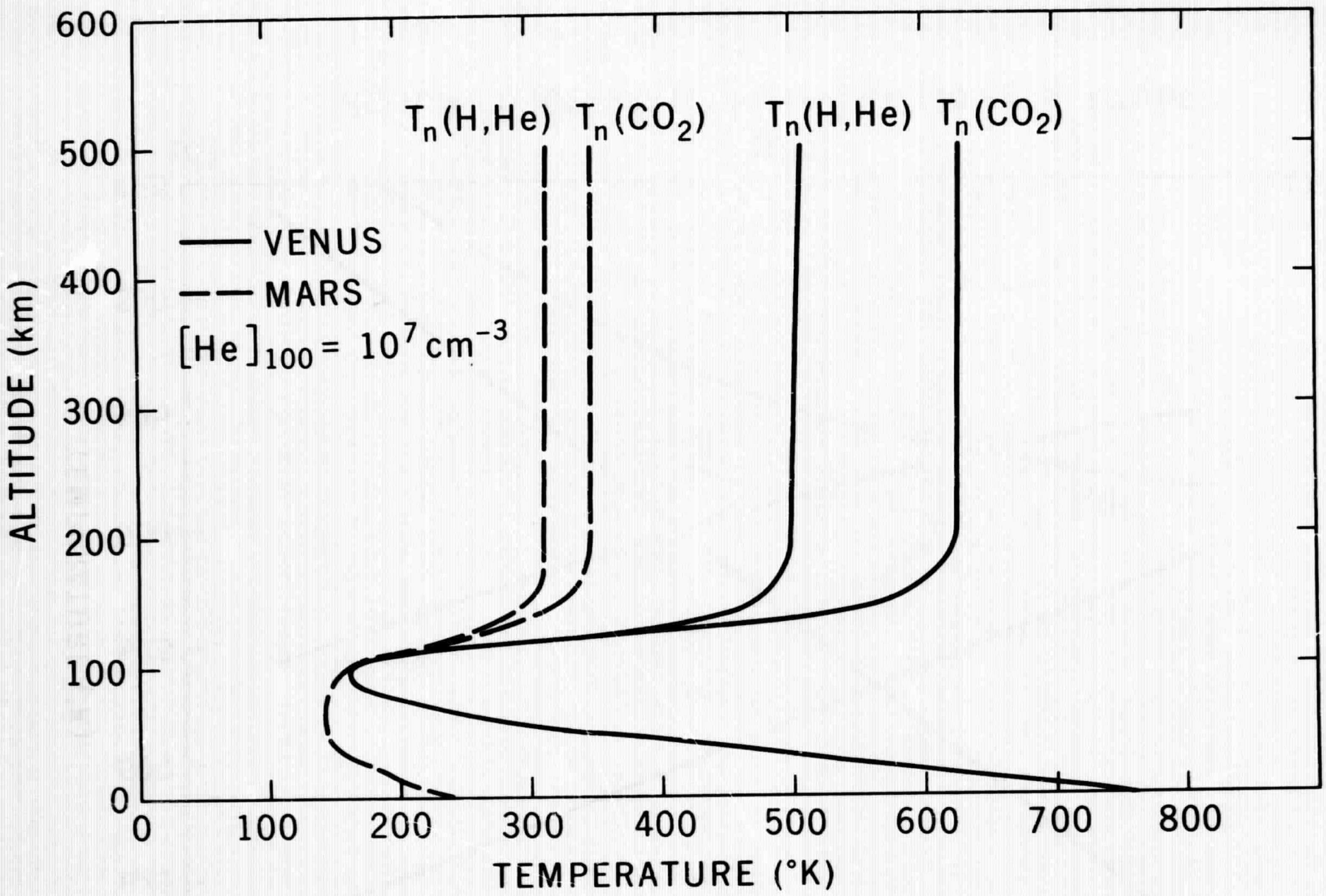

T_n(H,He) $T_n(CO_2)$ T_n(H,He) $T_n(CO_2)$
VENUS
MARS
$[He]_{100} = 10^7 cm^{-3}$
ALTITUDE (km)
TEMPERATURE (°K)

Figure 3

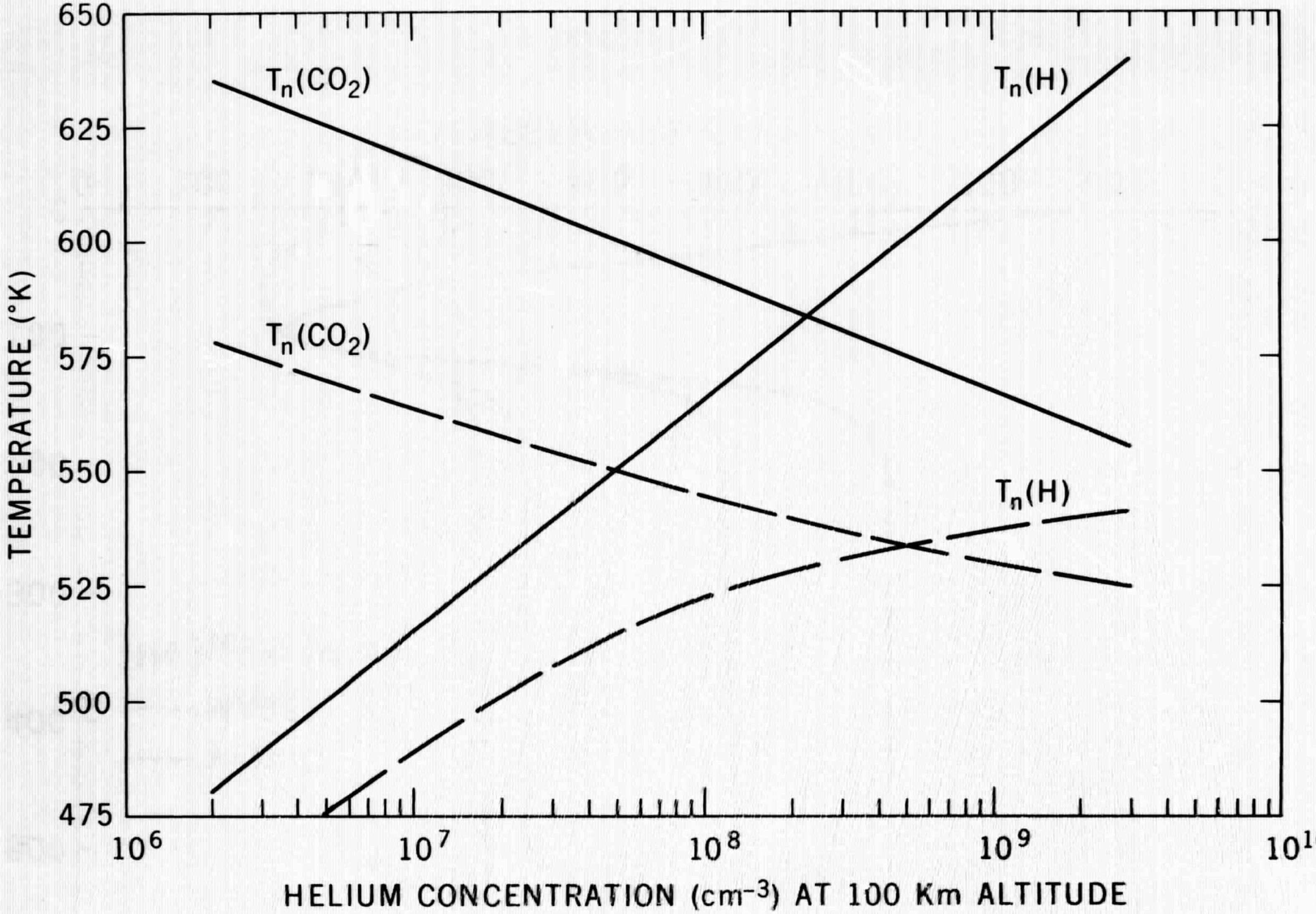

650
625
600
575
550
525
500
475
TEMPERATURE (°K)
$T_n(CO_2)$
$T_n(H)$
$T_n(CO_2)$
$T_n(H)$
10^6
10^7
10^8
10^9
10^{10}
HELIUM CONCENTRATION (cm^{-3}) AT 100 Km ALTITUDE

Figure 4

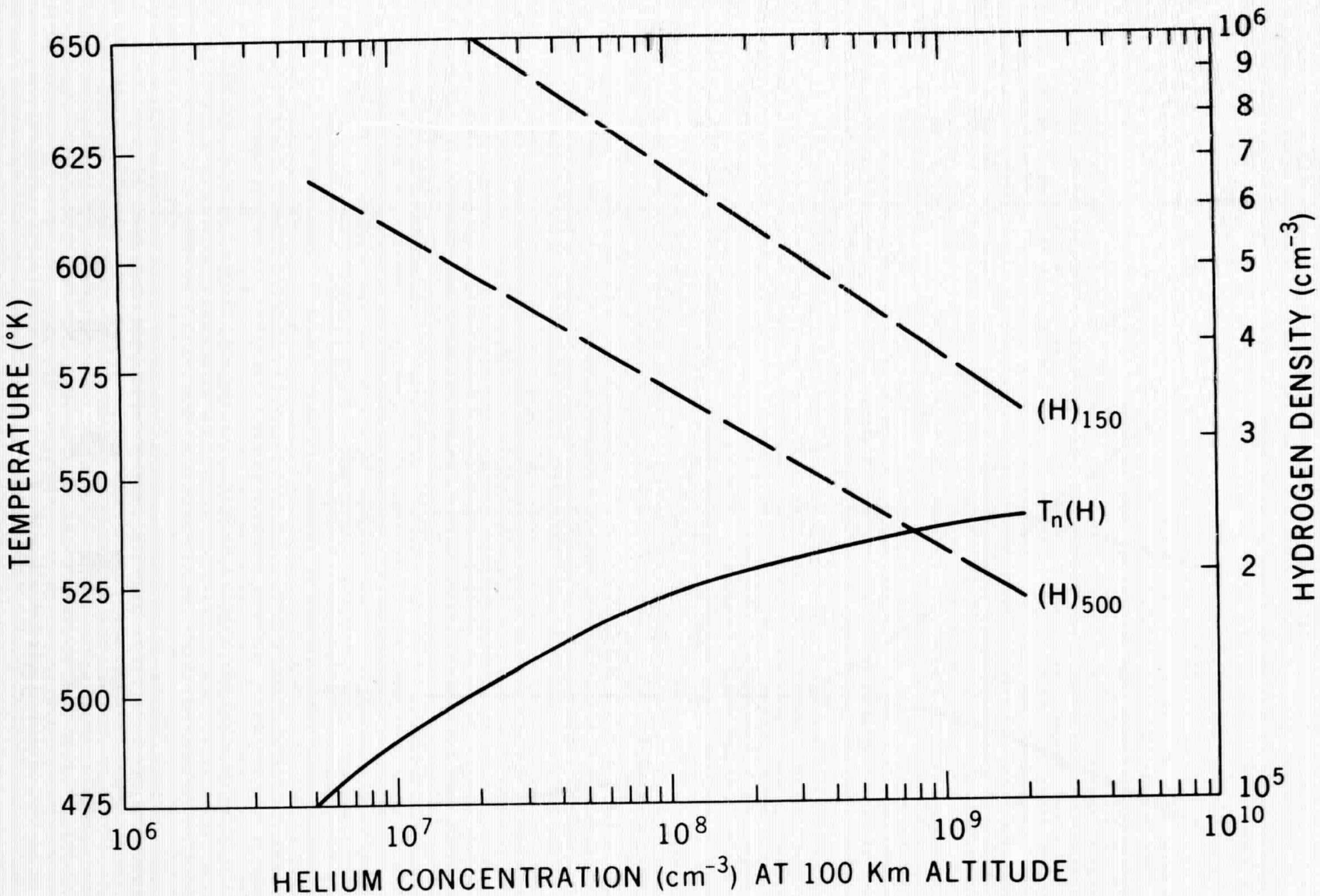

650
625
600
575
550
525
500
475
TEMPERATURE (°K)
10^6
9
8
7
6
5
4
3
2
10^5
HYDROGEN DENSITY (cm^{-3})
$(H)_{150}$
$T_n(H)$
$(H)_{500}$
10^6
10^7
10^8
10^9
10^{10}
HELIUM CONCENTRATION (cm^{-3}) AT 100 Km ALTITUDE

Figure 5

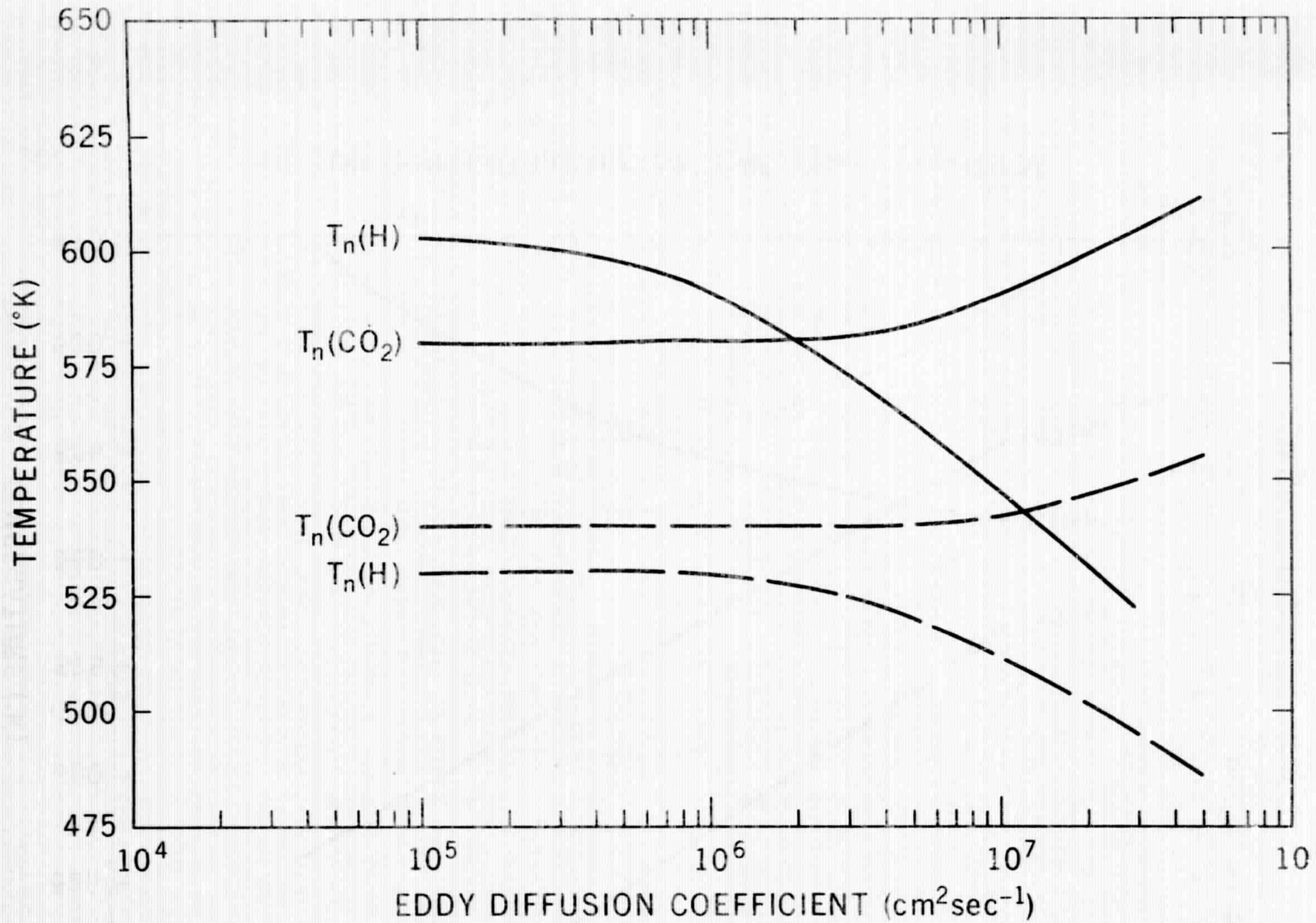

650
625
600
575
550
525
500
475
TEMPERATURE (°K)
$T_n(H)$
$T_n(CO_2)$
$T_n(CO_2)$
$T_n(H)$
10^4
10^5
10^6
10^7
10^8
EDDY DIFFUSION COEFFICIENT ($cm^2 sec^{-1}$)

Figure 6

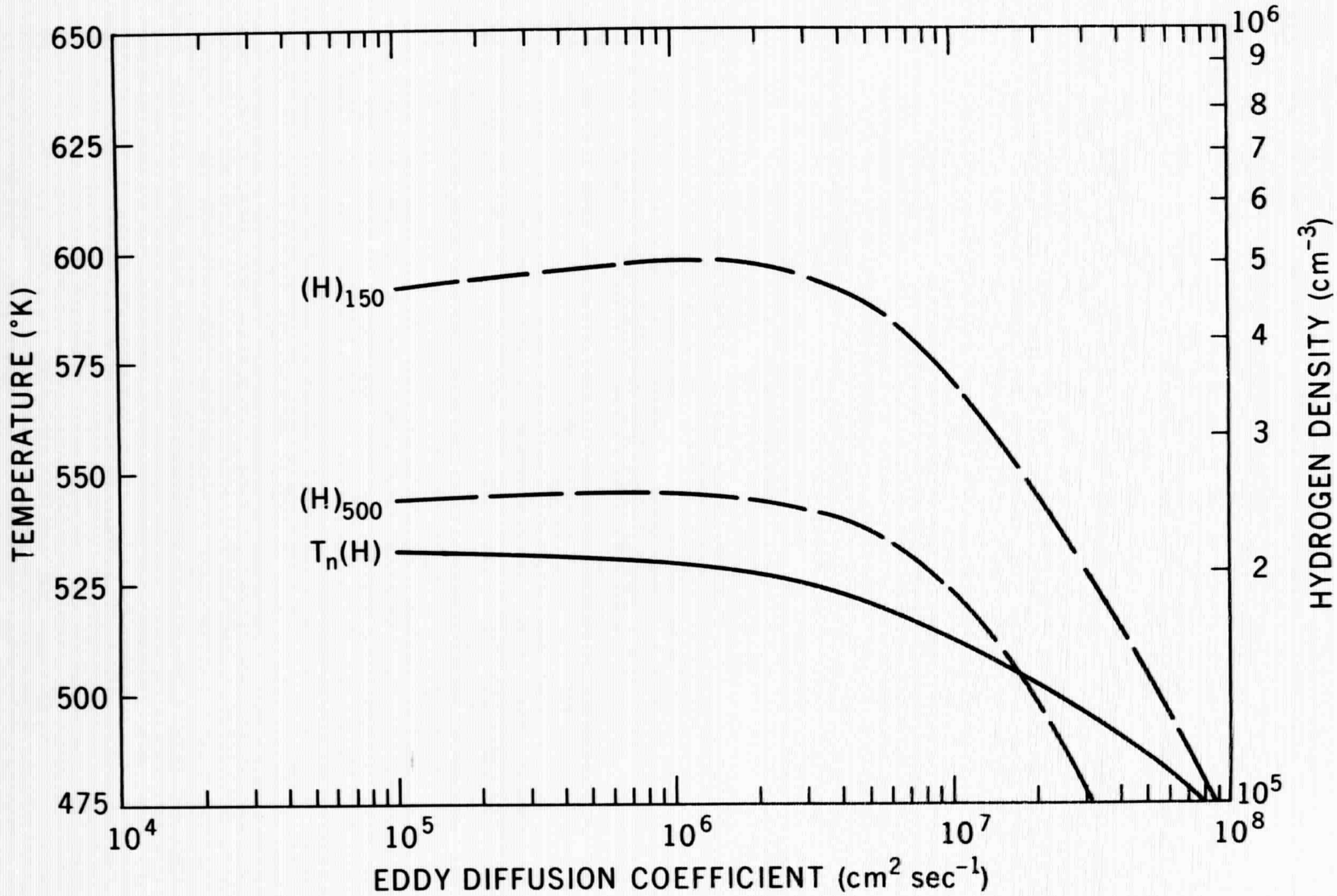

TEMPERATURE (°K)
650
625
600
575
550
525
500
475
HYDROGEN DENSITY (cm^{-3})
10^6
9
8
7
6
5
4
3
2
10^5
(H)$_{150}$
(H)$_{500}$
T_n(H)
10^4
10^5
10^6
10^7
10^8
EDDY DIFFUSION COEFFICIENT (cm^2 sec^{-1})

Figure 7